



Published in final edited form as:

Science. 1999 December 10; 286(5447): 2176–2179.

Mouse Tumor Model for Neurofibromatosis Type 1

Kristine S. Vogel^{1,*†}, Laura J. Klesse^{1,*}, Susana Velasco-Miguel^{1,*}, Kimberly Meyers^{1,*}, Elizabeth J. Rushing², and Luis F. Parada^{1,‡}

¹ Center for Developmental Biology, University of Texas Southwestern Medical Center, 6000 Harry Hines Blvd., Dallas, TX 75235–9133, USA

² Department of Pathology, University of Texas Southwestern Medical Center, 6000 Harry Hines Blvd., Dallas, TX 75235–9133, USA

Abstract

Neurofibromatosis type 1 (NF1) is an autosomal dominant disorder characterized by increased incidence of benign and malignant tumors of neural crest origin. Mutations that activate the protooncogene *ras*, such as loss of *Nf1*, cooperate with inactivating mutations at the *p53* tumor suppressor gene during malignant transformation. One hundred percent of mice harboring null *Nf1* and *p53* alleles in cis synergize to develop soft tissue sarcomas between 3 and 7 months of age. These sarcomas exhibit loss of heterozygosity at both gene loci and express phenotypic traits characteristic of neural crest derivatives and human NF1 malignancies.

Mutations in tumor suppressor genes are common events in human cancers (1). Individuals with a mutation in one copy of the *NF1* gene develop benign cutaneous neurofibromas, plexiform neurofibromas, café-au-lait spots, and axillary freckling (2). Through loss of heterozygosity (LOH) at the *NF1* locus, patients with neurofibromatosis type 1 are at increased risk of developing malignancies of neural crest derivatives, including malignant peripheral nerve sheath tumors (MPNSTs), malignant Triton tumors (MTTs), and pheochromocytomas (2,3). MPNSTs and MTTs arise from plexiform neurofibromas and frequently are associated with mutation or loss of the *p53* tumor suppressor gene (2,4). The protein product of the *NF1* gene neurofibromin is a guanosine triphosphatase (GTPase)–activating protein (GAP) that can negatively regulate p21ras signaling (5). Mutations that activate Ras cooperate with mutations that inactivate p53 in a number of transformation assays and models of tumorigenesis (6).

The *Nf1* and *p53* genes are linked in humans and in mice (7). To determine whether null mutations in *Nf1* and *p53* cooperate to accelerate tumorigenesis in vivo, we generated a recombinant mouse strain harboring inactivated *Nf1* and *p53* alleles linked on mouse chromosome 11. We accomplished this with intercrosses of trans-*Nf1*^{+/-}:*p53*^{+/-} compound heterozygotes or through crosses with *p53*^{+/-} heterozygotes. The integrity of the recombinant cis-*Nf1*:*p53* chromosome was established by genomic Southern blot analysis and by polymerase chain reaction (PCR). All progeny of cis-*Nf1*^{+/-}:*p53*^{+/-} test crosses to wild-type animals were either compound heterozygotes or entirely wild type, which confirms the integrity of the double-mutant chromosome.

‡To whom correspondence should be addressed. parada@utsw.swmed.edu.

*These authors contributed equally to this work.

†Present address: Department of Cell Biology and Anatomy, Louisiana State University Medical Center, New Orleans, LA 70112, USA.

Mice that are heterozygous for the *Nf1* mutation alone are at increased risk of developing pheochromocytomas and myeloid leukemias between 18 and 28 months of age (8). Loss of one or both copies of the *p53* gene leads to accelerated tumorigenesis. Thus, $p53^{-/-}$ mice develop lymphomas and hemangiosarcomas by 6 months of age, whereas $p53^{+/-}$ mice exhibit a predominance of osteosarcomas that arise later, after 9 months (9). We compared the mortality of trans- and cis- $Nf1^{+/-};p53^{+/-}$ compound heterozygotes with that of $p53^{+/-}$ and $p53^{-/-}$ mice on a mixed C57BL/6/129sv background (Fig. 1A). In addition, we analyzed survival of the null *p53* genotype together with *Nf1* heterozygosity (cis- $Nf1^{+/-};p53^{-/-}$). Introduction of one null *Nf1* allele accelerated tumor formation and mortality in the context of both the $p53^{+/-}$ and the $p53^{-/-}$ backgrounds (Fig. 1A). Both cis- and trans- $Nf1;p53$ mice developed tumors (primarily sarcomas) and died at 15 and 25 weeks, respectively, whereas the $p53^{+/-}$ mice survived beyond 37 weeks of age. Similarly, $Nf1^{+/-};p53^{-/-}$ mice began to develop tumors (primarily lymphomas) and die as early as 3 weeks of age, whereas $p53^{-/-}$ mice did not develop lymphomas before 18 weeks. Mice homozygous for the *p53* and the *Nf1* mutations are embryonic lethal and exhibit a high incidence of exencephaly (10).

To determine whether LOH had occurred at both loci in the cis- $Nf1;p53$ tumors, we used PCR-based assays to identify the wild-type and *neo*-disrupted alleles (9,11). As shown in Fig. 1B, 22 of 31 (71%) of the soft tissue sarcomas exhibited LOH at both loci; however, this may be an underestimate because of the difficulties of isolating pure tumor cells from surrounding normal tissue. Lymphomas isolated from trans- $Nf1^{+/-};p53^{+/-}$ and cis- $Nf1^{+/-};p53^{-/-}$ mice did not exhibit LOH at the *Nf1* locus (Fig. 1B, tumor 4).

To determine whether introduction of the *Nf1* mutation altered the tumor spectrum in cis- $Nf1;p53$ mice, we examined the pathological and phenotypic characteristics of the tumors. Histological analysis revealed that the cis- $Nf1^{+/-};p53^{+/-}$ mice exhibited a significant incidence of soft tissue sarcomas that appeared to be malignant based on their dedifferentiated morphology, disrupted tissue organization, and increased number of mitotic figures. Of 66 characterized tumors, 51 (77%) were sarcomas, 9 (14%) were lymphomas, 10 (8%) were carcinomas, and 2 were neuroblastomas. We subjected the soft tissue sarcomas to further analyses with antibodies specific for myoglobin, desmin, S100, and smooth muscle markers. On the basis of histopathological criteria and immunohistochemical analysis, we classified 11 tumors as MTTs, 31 as MPNSTs, 2 as leiomyosarcomas, 5 as rhabdomyosarcomas, and 4 as malignant fibrohistiocytomas (Fig. 1C). At least 3 of these malignant tumor types—MTTs, MPNSTs, and leiomyosarcomas—occur with increased frequency in human NF1 patients (2). Thus, the presence of the *Nf1* mutation, which alone is weakly tumorigenic, accelerates tumorigenesis and alters the tumor spectrum in the context of the $p53^{+/-}$ background.

Although NF1 is generally considered to be a neoplastic disorder of neural crest-derived cells, certain malignancies (rhabdomyosarcomas, leiomyosarcomas) have been associated with a mesodermal, rather than a neuroectodermal, origin (2). To address the origin of NF1 malignancies, we established permanent cell lines from over 70 independent cis- $Nf1;p53$ tumors. All tumor cell lines tested exhibited LOH at both *Nf1* and *p53* loci after only two or three passages in vitro to remove contaminating untransformed cells (Fig. 2A). As shown in Fig. 2B, reverse transcriptase (RT)-PCR analysis of representative cis- $Nf1;p53$ tumor cell lines revealed a spectrum of mRNAs encoding early neural crest and Schwann cell markers (12), including the transcription factor Pax-3, the low-affinity nerve growth factor (NGF) receptor p75, cell adhesion molecules N-CAM and L1, GAP-43, and the calcium binding protein S100. Many of the cell lines expressed mRNAs characteristic of more differentiated Schwann cells, including Krox-20 and the myelin-specific proteins P0 and myelin basic protein (12). In addition to these glial markers, the MTT lines expressed mRNAs

characteristic of myogenic differentiation, including desmin, MyoD, SM-22, and calponin (12). Immunocytochemical and immunoblot analyses also demonstrated expression of p75, S100, GFAP, GAP-43, smooth muscle actin (SMA), calponin, neurofilament, and peripherin proteins in many of the cis-Nf1: p53 tumor cell lines (Table 1). Tumor cell lines isolated from p53^{-/-} sarcomas did not express proteins characteristic of Schwann cell or neuronal differentiation in these assays (Table 1). Taken together, these data suggest that cis-Nf1:p53 cell lines derive from a neural crest stem cell that can follow Schwann cell, smooth muscle, or autonomic neuronal differentiation pathways (13). Thus, although the sarcomas that arise in cis-Nf1:p53 mice may differ in precise pathological classification, molecular analyses of the tumor cell lines are consistent with a common neural crest, rather than mesodermal, origin.

Generation of mouse mutants at suspected tumor suppressor loci has provided important information about the underlying mechanisms of tumor formation (14). It has therefore been perplexing that the original knockouts of the *Nf1* gene, modeled after the most frequently observed genetic neoplastic disorder in humans, did not afford a useful model for the benign neurofibromas or the malignant neurofibrosarcomas in NF1 patients (8,11). A possible explanation is that the period of embryonic development, cell differentiation, and growth is significantly reduced in the mouse. This temporal difference may shorten the window of opportunity for acquisition of additional mutations within a given cell or reduce the size of the target cell population. Our data, and those of Cichowski and colleagues (15), indicate that an additional mutation in the *p53* tumor suppressor gene is required to predispose Nf1^{+/-} mouse neural crest-derived cells to malignant transformation. Moreover, our molecular and immunochemical analyses provide evidence that NF1-associated rhabdomyosarcomas and leiomyosarcomas may be of neural crest origin and provide a possible explanation for the development of MTTs. Cell lines isolated from MTTs express both Schwann cell and smooth muscle markers, often in the same tumor cell (16). The phenotype of these tumors is consistent with immortalization of a pluripotent neural crest stem cell, which under normal circumstances adopts a glial, smooth muscle, or neuronal fate (13). Throughout development and adulthood, specific combinations of tumor suppressor genes may cooperate to control proliferation, differentiation, and survival in different cell lineages.

Acknowledgments

Supported by NIH grant NS34296 and the National Neurofibromatosis Foundation (L.F.P.) and by a grant from the Cancer Association of Greater New Orleans (K.S.V.). We thank T. Jacks and colleagues for sharing unpublished results, S. Colvin and J. Richardson for early assistance with histopathology, and members of the Parada lab for helpful discussions.

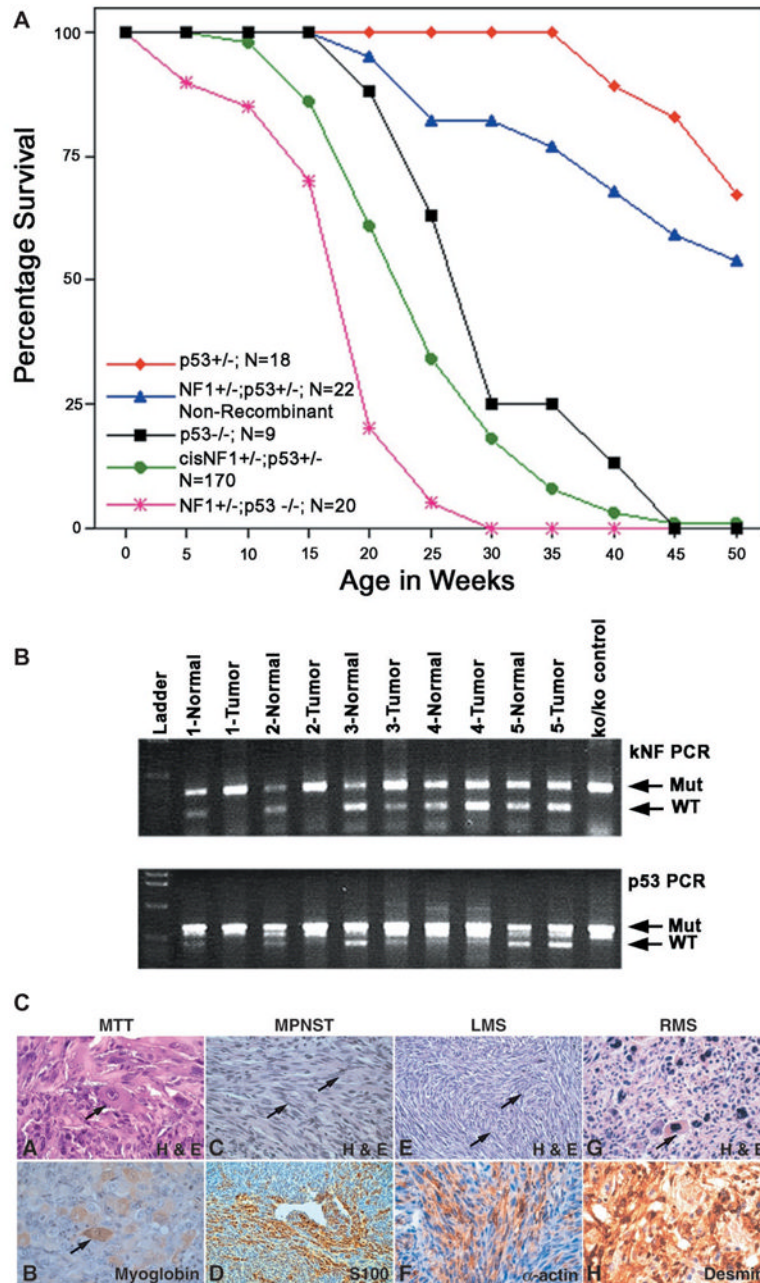
References and Notes

1. Hinds PW, Weinberg RA. *Curr Opin Genet Dev.* 1994; 4:135. [PubMed: 8193533] Knudson AG. *Proc Natl Acad Sci USA.* 1993; 90:10914. [PubMed: 7902574]
2. Bernardis V, et al. *Digestion.* 1999; 60:82. [PubMed: 9892804] Gutmann DH, et al. *JAMA.* 1997; 278:51. [PubMed: 9207339] Ishikazi Y, et al. *Surgery.* 1992; 111:706. [PubMed: 1595066] Riccardi VM, Womack JE, Jacks T. *Am J Pathol.* 1994; 145:994. [PubMed: 7977656]
3. Guha A, et al. *Oncogene.* 1996; 12:507. [PubMed: 8637706] Legius E, Marchuk DA, Collins FS, Glover TW. *Nature Genet.* 1993; 3:122. [PubMed: 8499945] Xu W, et al. *Genes Chromosomes Cancer.* 1992; 4:337. [PubMed: 1377942]
4. Halling KC, et al. *Anat Pathol.* 1996; 106:282. Jhanwar SC, Chen Q, Li FP, Brennan MF, Woodruff JM. *Cancer Genet Cytogenet.* 1994; 78:138. [PubMed: 7828144] Menon AG, et al. *Proc Natl Acad Sci USA.* 1990; 87:5435. [PubMed: 2142531]

5. Ballester R, et al. *Cell*. 1990; 63:851. [PubMed: 2121371] Buchberg AM, Cleveland LS, Jenkins NA, Copeland NG. *Nature*. 1990; 347:291. [PubMed: 2169593] Martin GA, et al. *Cell*. 1990; 63:843. [PubMed: 2121370] Xu GF, et al. *Cell*. 1990; 62:599. [PubMed: 2116237]
6. Eliyahu D, Raz A, Gruss P, Givol D, Oren M. *Nature*. 1984; 312:646. [PubMed: 6095116] Hundley JE, et al. *Mol Cell Biol*. 1997; 17:723. [PubMed: 9001226] Kemp CJ, Burns PA, Brown K, Nagase H, Balmain A. *Cold Spring Harbor Symp Quant Biol*. 1994; 54:427. [PubMed: 7587097] Parada LF, Land H, Weinberg RA, Wolf D, Rotter V. *Nature*. 1984; 312:649. [PubMed: 6390217] Tanaka M, Omura K, Watanabe Y, Oda Y, Nakanishi I. *J Surg Oncol*. 1994; 57:57. [PubMed: 7914949]
7. Copeland NG, et al. *Science*. 1993; 262:57. [PubMed: 8211130]
8. Jacks T, et al. *Nature Genet*. 1994; 7:353. [PubMed: 7920653]
9. Donehower LA, et al. *Nature*. 1992; 356:215. [PubMed: 1552940] Jacks T, et al. *Curr Biol*. 1994; 4:1. [PubMed: 7922305]
10. Vogel KS, Parada LF. *Mol Cell Neurosci*. 1998; 11:19. [PubMed: 9608530]
11. Brannan CI, et al. *Genes Dev*. 1994; 8:1019. [PubMed: 7926784]
12. Kioussi C, Gruss P. *Trends Genet*. 1996; 12:84. [PubMed: 8868344] Stemple DL, Anderson DJ. *Cell*. 1992; 71:973. [PubMed: 1458542]
13. Morrison SJ, White PM, Zock C, Anderson DJ. *Cell*. 1999; 96:737. [PubMed: 10089888] Shah NM, Groves AK, Anderson DJ. *Cell*. 1996; 85:331. [PubMed: 8616889]
14. Fero ML, Randel E, Gurley KE, Roberts JM, Kemp CJ. *Nature*. 1998; 396:177. [PubMed: 9823898] Giovannini M, et al. *Genes Dev*. 1999; 13:978. [PubMed: 10215625] Jacks T. *Annu Rev Genet*. 1996; 30:603. [PubMed: 8982467] Kamijo T, Bodner S, van de Kamp E, Hrandle D, Sherr CJ. *Cancer Res*. 1999; 59:2217. [PubMed: 10232611] McClatchey AI, et al. *Genes Dev*. 1998; 12:1121. [PubMed: 9553042] Orlow I, et al. *Int J Oncol*. 1999; 15:17. [PubMed: 10375589] Prolla TA, et al. *Nature Genet*. 1998; 18:276. [PubMed: 9500552] Zhu Y, Richardson JA, Parada LF, Graff JM. *Cell*. 1998; 94:703. [PubMed: 9753318]
15. Cicowski K, et al. *Science*. 1999; 286:2172. [PubMed: 10591652]
16. Vogel KS. unpublished data.
17. Nf1^{+/-};p53^{+/-} and Nf1^{+/-};p53^{-/-} progeny of trans-Nf1^{+/-};p53^{+/-} crosses were bred with mice that were wild type at both loci. A founder male with the genotype Nf1^{+/-};p53^{-/-} proved to harbor a stable recombinant chromosome 11 after test crosses to three wild-type females. The recombinant (cis configuration) chromosome was maintained on a mixed C57B6/129sv background, as were mice of other genotypes used for mortality studies. For genotyping, tail DNA was subjected to two separate three-primer PCRs, one for Nf1 (*11*) and one for p53 (*8*). Samples of macroscopically recognizable tumor were fixed in 10% buffered formalin, embedded in paraffin, and stained with hematoxylin and eosin. All immunostaining was done at room temperature on a BioTek Solutions Techmate automated immunostainer (Ventana BioTek Systems, Tucson, AZ). Buffers, blocking solutions, secondary antibodies, avidin-biotin complex reagents, chromogen, and hematoxylin counterstain were used as supplied in the Chem-Mate secondary detection kit (Ventana BioTek Systems). Optimum primary antibody dilutions were predetermined with known positive control tissues. A known positive control section was included in each run to ensure proper staining. Paraffin sections were cut at 3 μm on a rotary microtome and mounted on positively charged glass slides (POP100 capillary gap slides; Ventana BioTek Systems) at pH 6.8. Sections were incubated in unlabeled blocking antibody solution for 5 to 10 min to block nonspecific binding of secondary antibody and then incubated for 25 min with either primary antibody (S100 protein; SMA, 1:400; myoglobin, 1:60,000; desmin, 1:100; DAKO, Carpinteria, CA) or with buffer alone as a negative reagent control. After washing in buffer, sections were incubated for 25 min with biotinylated polyvalent secondary antibody solution (containing goat antibodies to rabbit, mouse, and rat immunoglobulin). After another buffer wash, sections were incubated with three changes, 2.5 min each, of 3% H₂O₂ to inhibit endogenous tissue peroxidase activity and again washed in buffer. Sections were then incubated for 25 min with freshly prepared horseradish peroxidase-conjugated avidin-biotin complex. Sections were then washed in buffer and incubated with three changes, 5 min each, of a freshly prepared mixture of diaminobenzidine (DAB) and H₂O₂ in buffer, followed by washing in buffer and then water. Sections were then counterstained with hematoxylin, dehydrated in a graded series of ethanols and xylene, and coverslipped. Slides were reviewed by light microscopy. Positive reactions with DAB

were identified as a dark brown reaction product. Sections were photographed on a Nikon Optiphot microscope (Nikon Instruments, Melville, NY).

18. Characterization of soft tissue sarcomas in *cis-Nf1:p53* mice. Histopathological examination was performed on all tumors obtained from animals at the termination of the experiment. Soft tissue tumors were classified in accordance with 1994 World Health Organization criteria. Tumor masses were removed under sterile conditions and measured. Small pieces of tumor tissue were removed for histological processing, DNA isolation, and establishment of tumor cell lines. Tumor samples were fixed in either Bouin's fixative (for hematoxylin and eosin staining) or 10% formalin (for immunohistochemistry) and processed for paraffin embedding and sectioning at 5 to 7 μ m. Tumor sections were immunostained with S100 antibody (anti-S100) (Novocastra), anti-desmin (Signet), anti- α -actin (Boehringer), or anti-myoglobin (Signet) and visualized by the Vectastain Elite ABC peroxidase method (Vector). Tumor DNA was genotyped by three-primer PCRs as described above.
19. Nf1/p53 tumor-derived cell lines were isolated as follows: Overlying skin and hair were removed from the tumor mass and then the tumor mass immersed briefly in Dulbecco's phosphate-buffered saline and in a solution of penicillin and streptomycin (Gibco). Small pieces of the tumor mass were minced in Dulbecco's modified Eagle's medium (DMEM) [supplemented with 10% heat-inactivated fetal calf serum (HIFCS), penicillin and streptomycin, and nonessential amino acids] (Gibco) with watchmaker's forceps and fine curved scissors. Tumor pieces were allowed to attach to 60-mm plastic tissue culture dishes, and clonal cell lines were established from tumor outgrowths after four to six passages.
20. For immunocytochemistry, tumor cells grown on coverslips in 2% HIFCS/DMEM were fixed in 4% paraformaldehyde and exposed to antibodies diluted overnight at 4°C as follows: p75 (Chemicon), 1:200; *c-neu* (Santa Cruz), 1:200; GAP-43, 1:250; S100 (Novocastra), 1:200; GFAP (Santa Cruz), 1:200; SMA (Sigma), 1:400; calponin (Sigma), 1:400; neurofilament (Chemicon), 1:200. To visualize bound antibody, we used Vectastain Elite ABC peroxidase kits (Vector Laboratories), specific for goat, rabbit, or mouse primary antibodies, according to the manufacturer's instructions. We also tested all primary antibodies with Cy3- or fluorescein isothiocyanate-conjugated fluorescent secondary antibodies (Chemicon, Sigma) to determine which method yielded little or no background staining. For immunoblots, proteins were extracted from tumor cells grown in 162-cm² culture flasks in Nonidet P-40 lysis buffer containing protease inhibitors (Sigma). Insoluble (SMA, GFAP) and soluble (*c-neu*, S100) fractions were subjected to SDS-polyacrylamide gel electrophoresis on 8% to 10% minigels. After protein transfer, nitrocellulose membranes were blocked with 2% bovine serum albumin in tris-buffered saline and incubated with primary antibody overnight at 4°C. Specific protein bands were visualized with Vectastain Elite ABC peroxidase kits (Vector Laboratories), or with Immun-Star kits (Bio-Rad), according to the manufacturers' instructions.

**Fig. 1.**

(A) Mice were maintained in specific pathogen-free conditions and observed daily for evidence of illness or tumor formation. If palpable tumors exceeded 1 cm in diameter or interfered with feeding and grooming, mice were sacrificed. Moribund mice with possible internal tumors were also sacrificed. Purple, $Nf1^{+/-};p53^{-/-}$; green, $cis-Nf1^{+/-};p53^{+/-}$ (17); black, $p53^{-/-}$; blue, $trans-Nf1^{+/-};p53^{+/-}$; red, $p53^{+/-}$. (B) PCR assay for wild-type (WT) and mutant (Mut) alleles of the *Nf1* and *p53* genes (8,11). Alternating lanes show normal and tumor tissue from five different mice. Tumors 1, 2, and 3 are *cis-Nf1:p53* sarcomas. Tumors 1 and 2 show LOH at both loci, whereas tumor 3 shows LOH at *p53* and reduced WT *Nf1*. Tumor 4 is an $Nf1^{+/-};p53^{-/-}$ lymphoma, and the mutant *p53* allele is present in normal and tumor tissues. No LOH was observed at the *Nf1* locus. Tumor 5 is a *cis-Nf1:p53* tumor that

did not show LOH at either locus. (C) Tumor histopathology and immunohistochemistry. (A) MTT. Rhabdomyoblastic cells stained with hematoxylin and eosin (H & E) (arrow) with abundant eosinophilic cytoplasm ($\times 20$). (B) Strong immunostaining of these cells with myoglobin ($\times 40$). (C) MPNST. H & E staining showing areas of typical intersecting fascicles of spindle-shaped cells (arrows) ($\times 20$). (D) Lower magnification ($\times 5$) shows intense S100 nuclear protein immunostaining of cells that surround branching vascular spaces. (E) Leiomyosarcoma (LMS) composed of intersecting horizontal and vertical (arrows) fascicles of spindle cells ($\times 5$). (F) Robust α -actin (SMA) immunostaining of LMS ($\times 10$). (G) Rhabdomyosarcoma (RMS) showing pleomorphic rhabdomyoblasts (arrow) intermingled with small polygonal cells ($\times 10$). (H) Desmin immunolabels mostly rhabdomyoblasts ($\times 20$). Methods are described in (18).

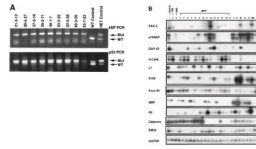


Fig. 2.

Expression of neural crest markers and LOH in cis-Nf1:p53 tumor cell lines (19). **(A)** DNAs from nine representative tumor lines that included MPNST, MTT, RMS, and LMS were assessed for LOH at Nf1 and p53. All tumor cell lines had complete LOH at both genes. Wild-type and heterozygous controls are shown for comparison. **(B)** Semiquantitative RT-PCR analysis of RNA obtained from representative cis-Nf1/p53 tumor-derived cell lines. Normal tissue samples from liver (L), heart (H), brain (B), kidney (K), spleen (S), skeletal muscle (SM), and NIH 3T3 fibroblasts (F) were used as controls. Samples lacking RT in the reaction mixture (–) were used as a negative control. Expression of the housekeeping gene GAPDH (GenBank accession no. M32599) was used as a loading control. Pax-3, paired box domain transcription factor (GenBank accession no. X59358); p75-NGF, NGF low-affinity receptor (GenBank accession no. X05137); GAP-43, growth-associated protein 43 (GenBank accession no. M16228); N-CAM, neural cell adhesion molecule (GenBank accession no. X15052); L1, immunoglobulin-related adhesion molecule (GenBank accession no. X12875); S100, calcium binding S100 protein (GenBank accession no. L22144); Krox-20, serum response zinc finger protein (GenBank accession no. X06746); MBP, myelin basic protein (GenBank accession no. M15060); P0, myelin P0 protein precursor (GenBank accession no. M62857); calponin (GenBank accession no. Z19542); SM22, smooth muscle protein 22 (GenBank accession no. 1351075) (19).

Table 1

Expression of neural crest, Schwann cell, smooth muscle, and neuronal markers in cis-Nf1: p53 tumor cell lines. Up to 41 tumor cell lines isolated from 10 cis-Nf1:p53 sarcomas were processed for immunocytochemistry. Immunostaining patterns for SMA, S100, GFAP, and *c-neu* were confirmed by immunoblot analysis (20). Four control cell lines were isolated from two Nf1^{+/+}: p53^{-/-} sarcomas; all four were positive for smooth muscle markers SMA and calponin but negative for glial, neuronal, and neural crest markers. +++, Strong immunostaining; ++, moderate immunostaining; +, weak immunostaining; -, no detectable immunostaining.

Marker	+++	++	+	-
p75	0/6	2/6	4/6	0/6
<i>c-neu</i>	2/10	8/10	0/10	0/10
GAP-43	0/6	3/6	3/6	0/6
S100	0/36	15/36	20/36	1/36
GFAP	0/21	0/21	13/21	8/21
SMA	3/41	27/41	11/41	0/41
Calponin	4/35	23/35	8/35	0/35
Neurofilament	1/34	4/34	7/34	22/34